TUMORIGENESIS AND NEOPLASTIC PROGRESSION

Loss of *Lrig1* Leads to Expansion of Brunner Glands Followed by Duodenal Adenomas with Gastric Metaplasia

CrossMark

Yang Wang,* Chanjuan Shi,[†] Yuanyuan Lu,* Emily J. Poulin,[‡] Jeffery L. Franklin,[‡] and Robert J. Coffey*[‡§]

From the Departments of Medicine, Pathology, Microbiology, and Immunology,[†] and Cell and Developmental Biology,[‡] Vanderbilt University Medical Center, Nashville; and the Department of Veterans Affairs Medical Center,[§] Nashville, Tennessee*

Leucine-rich repeats and immunoglobulin-like domains 1 (LRIG1) is a pan-ErbB negative regulator and intestinal stem cell marker down-regulated in many malignancies. We previously reported that 14 of 16 *Lrig1-CreERT2/CreERT2* (*Lrig1*^{−/−}) mice developed duodenal adenomas, providing the first *in vivo* evidence that Lrig1 acts as a tumor suppressor. We extended this study to a larger cohort and found that 49 of 54 *Lrig1*^{−/−} mice develop duodenal adenomas beginning at 3 months. Most adenomas were histologically low grade and overlaid expanded Brunner glands. There was morphologic and biochemical blurring of the boundary between the epithelium and Brunner glands with glandular coexpression of ErbB2, which is normally restricted to the epithelium, and the Brunner gland marker Mucin6. Some adenomas were high grade with reduced Brunner glands. At age 4 to 5 weeks, before adenoma formation, we observed enhanced proliferation in Brunner glands and, at 2 months, an increase in the size of the Brunner gland compartment. Elevated expression of the epidermal growth factor receptor (Egfr) ligands amphiregulin and β-cellulin, as well as Egfr and phosphorylated Egfr, was detected in adenomas compared with adjacent normal tissue. These adenomas expressed the gastric-specific genes gastrokine1 and mucin5ac, indicating gastric metaplasia. Moreover, we found that a subset of human duodenal tumors exhibited features of *LRIG1*^{−/−} adenomas, including loss of LRIG1, gastric metaplasia (MUCIN5AC and MUCIN6), and increased amphiregulin and Egfr activity. (*Am J Pathol* 2015, 185: 1123−1134; http://dx.doi.org/10.1016/j.ajpath.2014.12.014)

The ERBB family of receptor tyrosine kinases includes epidermal growth factor receptor (EGFR, or ERBB1) and ERBB2-4.[1−3] Seven mammalian ligands bind EGFR: EGF, transforming growth factor-α, heparin-binding EGF-like growth factor, amphiregulin (AREG), epiregulin, beta-cellulin (BTC), and epigen.[4] ERBB signaling plays critical roles during the development and maintenance of homeostasis in adult tissues. Precise regulation of signaling is required to ensure the fidelity of these processes, especially because EGFR activation induces transcription of EGFR and its ligands in a positive feedback manner.[5,6] Loss of ERBB negative regulation as a mechanism of aberrant ERBB activation is beginning to be appreciated as a hallmark of cancers.[7,8]

Leucine-rich repeats and immunoglobulin-like domains 1 (LRIG1), a pan-ERBB negative regulator, is a transmembrane protein that down-regulates EGFR signaling by accelerating receptor internalization and degradation in a c-CBL−dependent manner.[9,10] Reduced expression of LRIG1 has been reported in breast,[11,12] cervical,[13] and skin cancers,[14] as recently reviewed by Wang et al[9] and Hedman and colleagues.[15] In addition, the soluble ectodomain of LRIG1 inhibits *in vivo* growth of EGFRVIII mutant gliomas,[16] and restoration of LRIG1 expression sensitizes glioma cells to chemotherapy.[17]

We recently showed that Lrig1 marks a distinct population of stem cells in the small and large intestines and that the genetic ablation of *Lrig1* resulted in duodenal adenomas in 14 of 16 mice.[18] We now show that 49 of 54 *Lrig1-CreERT2/CreERT2* (hereafter referred to as *Lrig1*$^{-/-}$) mice developed duodenal adenomas beginning at 3 months of age. Moreover, we provide a detailed histologic, molecular, and biochemical characterization of these adenomas. We found that loss of *Lrig1* results in highly penetrant duodenal adenomas with gastric metaplasia and increased ErbB signaling. In addition, we identified a subset of previously unrecognized human duodenal adenomas and carcinomas that also have dysplastic Brunner glands, gastric metaplasia, heightened EGFR signaling, and reduced LRIG1 immunoreactivity.

Materials and Methods

Animal Studies

The generation of *Lrig1*$^{tm1.1(cre/ERT)Rjc}$ (*Lrig1-CreERT2*) mice was described elsewhere.[18] *Lrig1*$^{-/-}$ (homozygous *Lrig1-CreERT2*) mice and wild-type littermates were maintained on a *129S7/SvEv* and *C57BL/6* mixed background. *Lrig1-CreERT2/CreERT2;RosaR26R-EYFP/EYFP* (cis) mice were obtained by intercrossing *Lrig1-CreERT2/+;RosaR26R-EYFP/+* (cis) mice. The *Lrig1* and *Rosa26R* loci are 18 Mb apart on chromosome 6. During extensive mating, a rare crossover event occurred, which resulted in the engineered loci residing in cis and cosegregating in subsequent progeny. I.P. injection of 2 mg of tamoxifen dissolved in corn oil at 4 weeks of age was used to initiate lineage tracing to assess the contribution of cells with *Lrig1* loss in tumorigenesis. Freshly dissected mouse duodenum was fixed in 4% paraformaldehyde overnight at 4°C, followed by dehydration and paraffin embedding. All the animal studies were approved by the Division of Animal Care at Vanderbilt University (Nashville, TN).

Human Tissues

Pathology slides of human duodenal/ampullary adenomas ($n = 27$, from 2007 to 2012) and adenocarcinomas ($n = 61$, from 1994 to 2012) from the Vanderbilt University pathology archives were reviewed. Five adenocarcinomas and three adenomas meeting the following criteria were further analyzed: occurring in the periampullary duodenum, presence of dysplastic Brunner glands, and CDX2 negativity by immunohistochemical (IHC) analysis. Use of human tissues was approved by the Vanderbilt University Institutional Review Board.

Histologic, IHC, and Immunofluorescence Analysis

Histologic analysis and immunostaining were performed on 5-μm sections. Briefly, antigen retrieval was performed in Target retrieval buffer (pH, 6; Dako, Carpinteria, CA) in an automated pressure cooker for 15 minutes on high pressure for all antibodies unless otherwise specified. For ErbB2 and phosphorylated EGFR (p-EGFR) IHC analysis, antigen retrieval was performed in Target retrieval buffer (pH, 9; Dako). For IHC analysis, anti-rabbit and anti-mouse polymers (Dako) were used for secondary antibody detection and peroxidase visualization.

For immunofluorescence, Alexa Fluor 488—conjugated or Alexa Fluor 568—conjugated goat—anti-rabbit/mouse secondary antibodies (Life Technologies, Grand Island, NY) were used for visualization. Primary antibodies included anti—p-EGFR pY1068 (dilution 1:500; Epitomics Inc., Burlingame, CA), anti-ERBB2 (dilution 1:700; Cell Signaling Technology Inc., Danvers, MA), anti-Muc6 (dilution 1:100; Kanto Chemical Co. Inc., Tokyo, Japan), anti-MUC6 (dilution 1:200; Novocastra, Buffalo Grove, IL), anti-Muc5ac (dilution 1:500; NeoMarkers, Fremont, CA), anti-MUC5AC (dilution 1:300; Thermo Scientific, Waltham, MA), anti-Gastrokine1 (dilution 1:500; Abcam Inc., Cambridge, MA), anti-AREG (dilution 1:100; Lab Vision, Fremont, CA), anti—Ki-67 (dilution 1:200;

Table 1 Quantitative RT-PCR Primer Information

Gene	Forward primer	Reverse primer
Areg	5′–AACGGTGTGGAGAAAAATCC–3′	5′–TTGTCCTCAGCTAGGCAATG–3′
Btc	5′–GTGTGGTAGCAGATGGGAAC–3′	5′–ATCTCCCATGGATGCAGTAA–3′
Hbegf	5′–GAGCAACAGAGCTGAGAAGC–3′	5′–TATTTTCCCCCTCTGGGTAG–3′
Ereg	5′–AACTGTTCACCAACCCTTGA–3′	5′–CCTTGTCCGTAACTTGATGG–3′
Egf	5′–TTGTTAGCACCATCCCTCAT–3′	5′–CGGGAGAGTTCTTTGTCTCA–3′
Tgfa	5′–CACTGGACTTCAGCCCTCTA–3′	5′–TCCAGCAGACCAGAAAAGAC–3′
Epn	5′–CCAATGGAGATCTTTGGATG–3′	5′–TCTTCCTGCAGTGACAACAA–3′
Egfr	5′–GTGATGGGGATGTGATCATT–3′	5′–AGCATAAAGGATTGCAGACG–3′
ErbB2	5′–GCCCTCATCACCTACAACAC–3′	5′–CTCAGCTGTGACCTCTTGGT–3′
ErbB3	5′–GGCTACGACTGGCTGAAATA–3′	5′–CGCTCTCTTGATGACCAGAT–3′
ErbB4	5′–GGACCCACAGAAAATCACTG–3′	5′–TGTTCCAGTTGAAAGGTGGT–3′
Tff1	5′–GGAGAGAGGTTGCTGTTTTG–3′	5′–TCTGAGGGGTTGAACTGTGT–3′
Tff2	5′–TGCTTTGATCTTGGATGCTG–3′	5′–GGAAAAGCAGCAGTTTCGAC–3′
Gkn1	5′–AGATTCCAGGACCAAACCAG–3′	5′–ACAACCCCCAGAGAACACTC–3′
Gkn2	5′–ACAGTGACCATCGACAACCA–3′	5′–AACCGTTGGAGTTTGTCCAG–3′
Gkn3	5′–AATACGGAGTGCCAATCAAA–3′	5′–ACACTTCTCACAGGCAGAGG–3′

Dako), anti-MUC2 (dilution 1:100; Santa Cruz Biotechnology, Dallas, TX), anti-Lrig1 (dilution 1:100; R&D Systems, Minneapolis, MN), anti-LRIG1 (dilution 1:100; Agrisera AB, Vännäs, Sweden), and anti-EGFP (dilution 1:500; Life Technologies).

To quantify Ki-67 positivity, all Ki-67$^+$ cells in Brunner glands were automatically counted by a Leica image viewer (Leica Microsystems GmbH, Wetzlar, Germany) and divided by the total number of Brunner glands in a given section. To measure the size of Brunner glands in mouse duodenum, approximately 2 cm of the very proximal duodenum (including approximately 0.5 cm of the antrum) was cut open longitudinally, fixed with 4% paraformaldehyde, and embedded on its edge in paraffin. For every 100-μm thickness, a 5-μm section was cut until tissue was exhausted. All the sections were hematoxylin and eosin stained and then scanned with an Ariol SL-50 automated scanning microscope (Leica Microsystems GmbH), with the area of the Brunner gland compartment manually drawn and calculated by Digital Image Hub software version 4.0.4 (Leica Microsystems GmbH). A section that encompassed the medial area was chosen from each animal to calculate the average size of Brunner glands from each genotype. Brightfield IHC images were scanned using the Leica SCN400 slide scanner (Leica Microsystems GmbH), and immunofluorescence images were either scanned using the Ariol SL-50 automated scanning microscope or taken with an Olympus FV1000 inverted confocal microscope (Olympus America Inc., Pittsburgh, PA).

Microarray Analysis and RT-qPCR

Full thicknesses of fresh duodenal adenoma (approximately 0.5 to 0.7 cm in longitudinal length), adjacent normal duodenum distal to adenoma (approximately 0.7 cm in longitudinal length), and wild-type proximal duodenum (approximately 0.7 cm in longitudinal length, equivalent to the position of adenomas in *Lrig1* null mice) were snap frozen in liquid nitrogen and ground using an electronic grinder (A. Daigger & Co. Inc., Vernon Hills, IL). Total RNA was extracted using an RNeasy micro kit (Qiagen Inc., Maryland, VA). Gene profiling was performed on Affymetrix Mouse Gene 1.0 ST Array (Affymetrix, Santa Clara, CA) by VANTAGE (Vanderbilt University). Microarray data have been deposited in the National Center for Biotechnology Information's Gene Expression Omnibus[19] (*http://www.ncbi.nlm.nih.gov/geo*; Accession number GSE64640). For quantitative RT-PCR (RT-qPCR), cDNA was generated using SuperScript II Reverse Transcriptase (Life Technologies). RT-qPCR was performed in triplicate on a StepOnePlus real-time PCR system (Applied Biosystems, Grand Island, NY) and repeated three times. Each 20-μL reaction contained 0.1 μmol/L primers, 4 mmol/L MgCl$_2$, and EXPRESS SYBR GreenER Supermix with premixed ROX (Life Technologies). RT-qPCR reactions were performed under the following conditions: 50°C for 2 minutes, 95°C for 2 minutes, followed by 40 cycles at 95°C for 15 seconds and 58°C for 45 seconds, after which a melting curve was
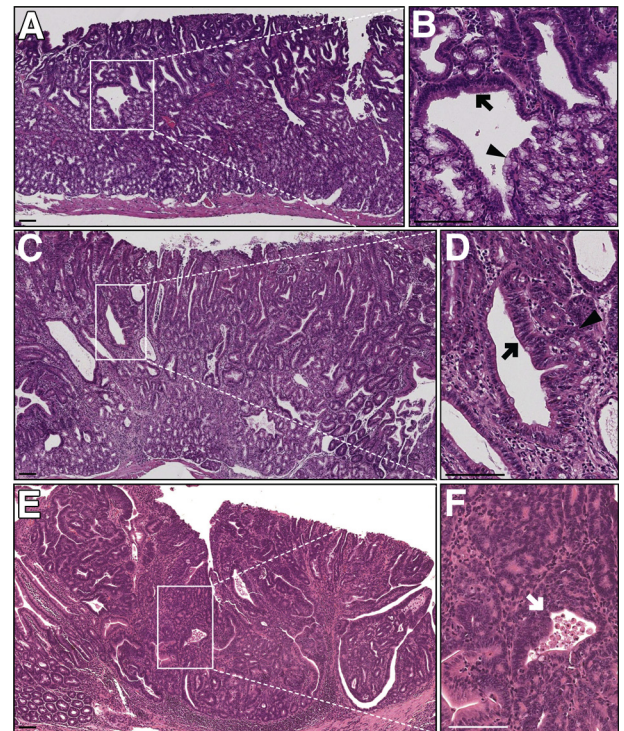
Figure 1 Representative histologic features of *Lrig1*$^{-/-}$ duodenal adenomas. **A:** Hematoxylin and eosin (H&E) staining of a less advanced duodenal adenoma from a 14-month-old *Lrig1*$^{-/-}$ mouse. The adenoma contained multiple cystically dilated glands and overlaid an expanded but histologically normal Brunner gland region. **B:** Magnification of the **boxed region** in **A** showing a blurring of the boundary between the overlying epithelium and Brunner glands, with features of both compartments in this transition zone. A cystically dilated gland containing both low-grade adenomatous features with nuclear enlargement and hyperchromasia (**black arrow**) and relatively normal Brunner gland cells (**black arrowhead**). **C:** H&E of an adenoma with more advanced dysplastic features from a 5-month-old *Lrig1*$^{-/-}$ mouse. The dysplastic cells extended deeper into the Brunner gland compartment. **D:** A high-power view of the **boxed region** in **C** showing an adenomatous gland with nuclear enlargement and an increased nuclear/cytoplasmic ratio (**black arrow**) with adjacent small adenomatous glands composed of cuboidal epithelium (**black arrowhead**). **E:** H&E of a high-grade adenoma from a 14-month-old *Lrig1*$^{-/-}$ mouse with increased cytologic atypia and greater architectural complexity. **F:** A high-power view of the **boxed region** in **E** showing back-to-back (cribriform) glands and a gland containing necrotic debris in its lumen (**white arrow**). Scale bars: 100 μm. Original magnification: ×3.8 (**B**).

performed to ensure the specificity of the PCR products. Results were analyzed using the $\Delta\Delta C_T$ method. All the primer sets (Table 1) except Tff2 (a gift from James R. Goldenring, Vanderbilt University Medical Center) were purchased from RealTimePCR.com (Cambridge, UK) and were validated using relative standard curve methods followed by a melting curve before applying to experimental samples.

Statistical Analysis

Data are presented as means ± SEM. The unpaired Student's *t*-test was used to determine statistical significance, with a cutoff value of $P < 0.05$. All the graphs and statistical analyses were performed using Prism 6 software (GraphPad Software Inc., San Diego, CA).
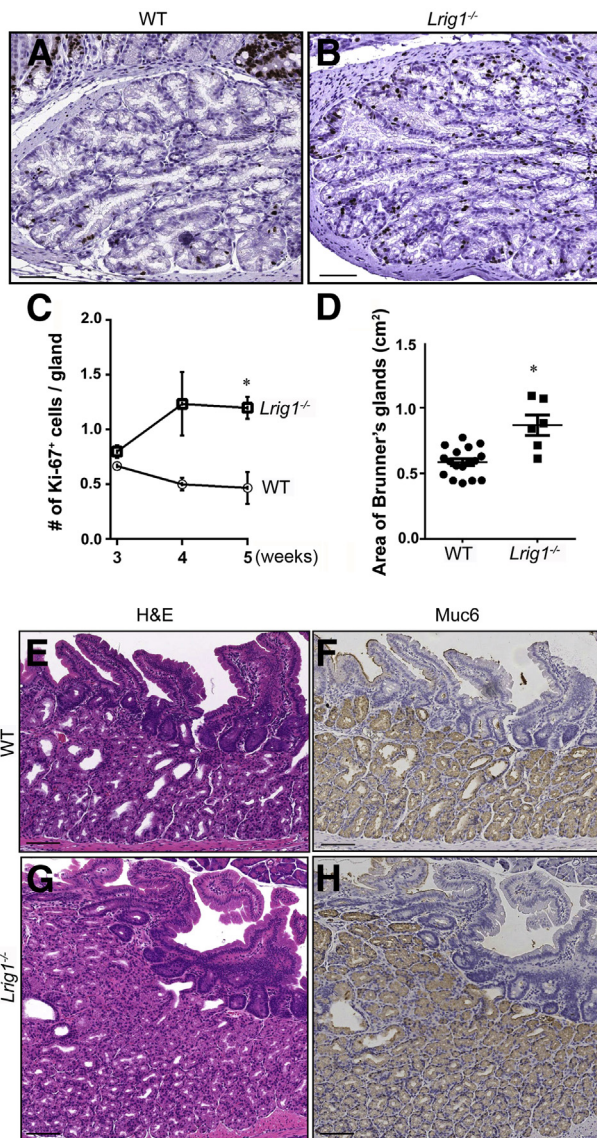
Figure 2 Loss of *Lrig1* promotes Brunner gland proliferation and expansion before adenoma formation. **A** and **B:** Ki-67 immunohistochemical analysis demonstrated significantly more proliferative cells in Brunner glands of a 4-week-old *Lrig1*^{−/−} mouse (**B**) compared with an age-matched wild-type (WT) mouse (**A**). **C:** The mean number of Ki-67^{+} cells per gland is similar at 3 weeks of age. This number increased at 4 and 5 weeks of age in *Lrig1*^{−/−} mice but decreased at these times in WT mice. **D:** The size of the Brunner gland compartment in 2-month-old *Lrig1*^{−/−} mice (*n* = 5) is 1.5-fold greater than that in age-matched WT mice (*n* = 10). **E** and **G:** Hematoxylin and eosin (H&E) demonstrates enlargement of the Brunner gland region in an *Lrig1*^{−/−} mouse compared with a WT control. **F** and **H:** Muc6 immunoreactivity is confined to Brunner glands in WT and *Lrig1*^{−/−} mice. Data are given as means ± SEM. *$P < 0.05$. Scale bars: 100 μm.

Results

Loss of Lrig1 Leads to Duodenal Adenomas Overlying an Expanded Brunner Gland Compartment

We previously reported that 14 of 16 *Lrig1*^{−/−} mice (88%) developed spontaneous duodenal adenomas.[18] Herein we extended this analysis to show that 49 of 54 *Lrig1*^{−/−} mice (91%) developed adenomas in the proximal duodenum, with adenomas first noted at 3 months of age. The histologic features of these adenomas vary; representative features are shown in Figure 1 and Supplemental Figure S1. Most of the adenomas were histologically low grade, overlying an expanded Brunner gland compartment (Figure 1, A and C). Cystically dilated glands were often seen (Figure 1, B and D). These lesions also contained cuboidal epithelial cells (Figure 1D). In low-grade lesions, the boundary between Brunner glands and the overlying epithelium was blurred, with a mixture of normal Brunner gland cells, cuboidal Brunner gland cells with nuclear enlargement, and slightly cuboidal cells with hyperchromatic nuclei and a higher nuclear/cytoplasmic ratio coexisting in the same gland in this transition zone
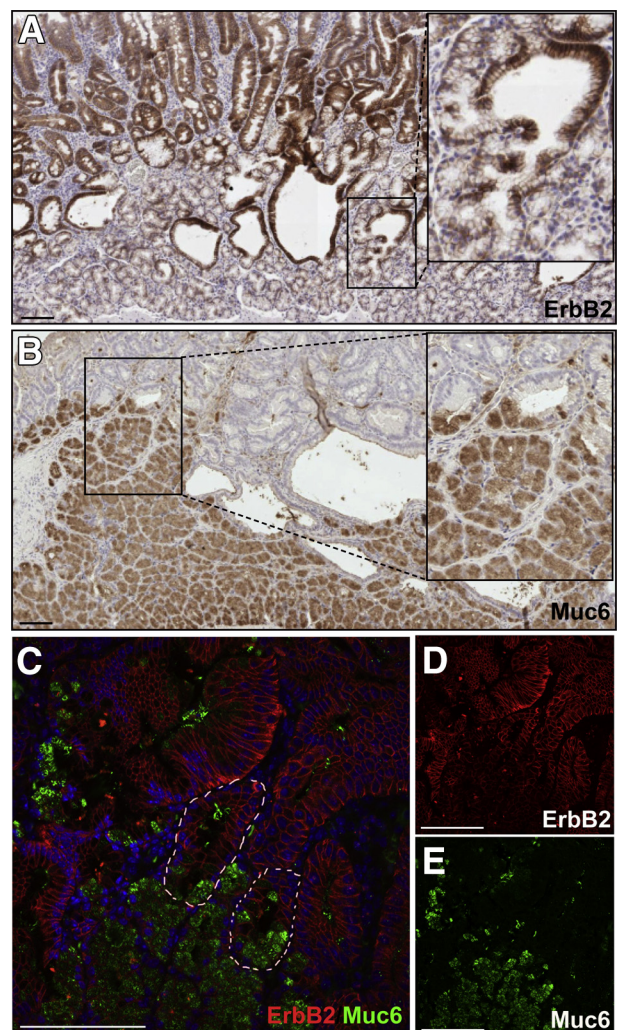
Figure 3 Blurring of the boundary between early adenoma and underlying Brunner glands. **A** and **B:** Immunohistochemical analysis for ErbB2 (**A**) in the overlying early adenoma and Muc6 (**B**) in Brunner glands. The transition zones between the two compartments are **boxed** and magnified in the **insets**. These glands show partial staining for ErbB2 and Muc6. **C:** Immunofluorescence shows co-staining for ErbB2 (red) and Muc6 (green) in the same glands (indicated by **white dashed lines**). **D** and **E:** Individual staining for ErbB2 and Muc6. Scale bars: 100 μm. Original magnification: ×2.5 (**insets, B** and **C**).

(Figure 1B). More advanced lesions exhibited increased basophilia, marked nuclear atypia, complex glandular architecture, and dysplastic glands with necrotic debris (Figure 1F); expansion of Brunner glands seemed less or completely absent in these advanced lesions (Figure 1E). Occasionally, lobules of histologically abnormal Brunner glands with larger nuclei and reduced mucin were observed (Supplemental Figure S1A). Tubular adenomas were sometimes found in the duodenum distal to Brunner glands (Supplemental Figure S1, B−D).

To study the pathogenesis of these duodenal adenomas, we examined the histologic features of the proximal duodenum before adenoma formation. In wild-type and *Lrig1*^{−/−} mice, Brunner glands were present at birth, and there was Ki-67 immunoreactivity throughout the glands (Figure 2, A and B, and data not shown). In wild-type mice, Ki-67 positivity, indicating actively dividing cells, decreased after 3 weeks of age (Figure 2C), and there was little, if any, Ki-67 immunoreactivity at 2 months (data not shown). Ki-67 immunoreactivity was similar in wild-type and *Lrig1*^{−/−} mice at 3 weeks of age (Figure 2C and Supplemental Table S1). However, the number of Ki-67^{+} positive cells was increased in *Lrig1*^{−/−} mice at 4 and 5 weeks of age; there were approximately threefold more Ki-67^{+} cells in *Lrig1*^{−/−} mice compared with wild-type mice at 5 weeks ($P < 0.05$) (Figure 2C). Therefore, these data suggest that Brunner gland proliferation persists in mice lacking *Lrig1* in early adulthood.

At 2 months of age, but not before, we observed a 1.5-fold increase in the size of Brunner glands in *Lrig1*^{−/−} mice compared with age-matched wild-type controls ($P < 0.05$) (Figure 2, D−H), presumably due to the heightened proliferation observed at 4 and 5 weeks of age. Brunner glands are secretory glands located in the submucosa of the proximal duodenum that secrete bicarbonate and mucin to neutralize acidic contents from the stomach. Brunner glands and the overlying epithelium form two histologically discrete compartments. Brunner glands contain acinar-like cells with small nuclei, whereas the overlying epithelium is composed of typical columnar epithelial cells with larger elongated nuclei. In the normal intestine, Muc6 was found exclusively in Brunner glands (Figure 2F), and ErbB2 staining was restricted to the overlying epithelium (Supplemental Figure S2B).[20] However, in less advanced lesions from *Lrig1*^{−/−} mice, ErbB2 and Muc6 were coexpressed in the same gland in this blurred boundary (Figure 3), suggesting abnormalities in epithelial lineage allocation. Of note, surface erosions were not observed in normal mucosa or in tumors of younger mice (Supplemental Figure S1E), suggesting that adenoma formation is not a reactive process to gastric acidity.

Lrig1 protein was expressed in overlying epithelium and Brunner glands (Figure 4A). When *Lrig1*^{−/−} mice on a *Rosa26R-EYFP* background (*Lrig1-CreERT2/CreERT2; Rosa26R-EYFP/EYFP*) were lineage traced with a single tamoxifen induction at 4 weeks of age, a significant portion of the duodenal adenoma displayed YFP immunoreactivity (Figure 4, B−D), suggesting that progenitor cells lacking *Lrig1* in both compartments contribute to adenoma formation.
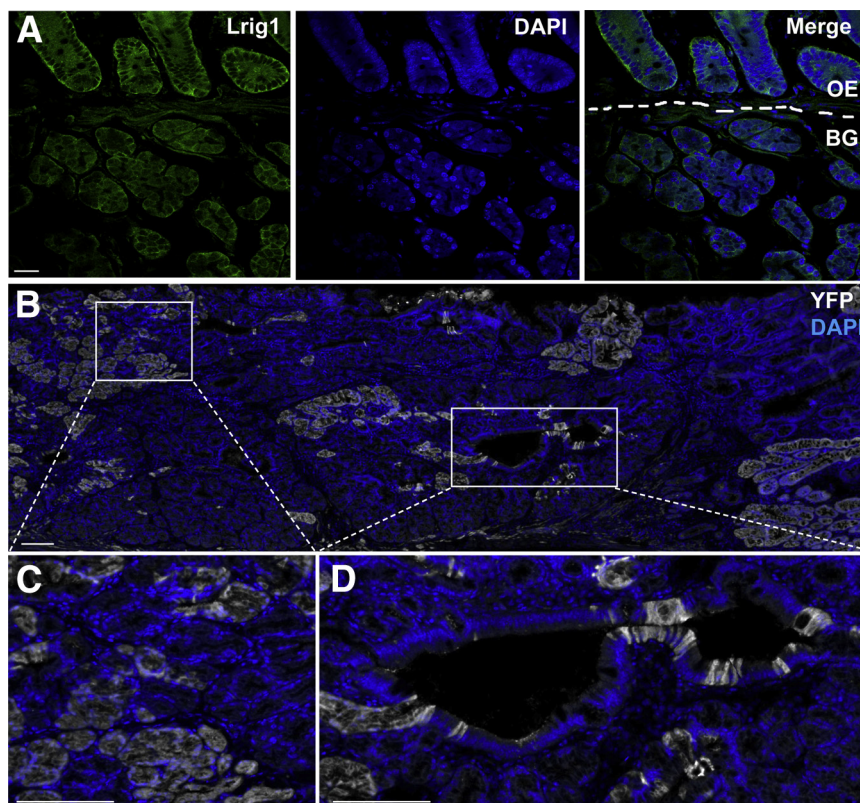
Figure 4 Lrig1 is expressed in both Brunner glands (BGs) and overlying epithelium (OE), and Lrig1^{+} cells contribute to tumorigenesis by lineage tracing. **A:** Immunofluorescence showing Lrig1 (green) expressed in BGs and OE (of which the two compartments were divided by **white dashed lines**). **B:** Green fluorescent protein (GFP) immunofluorescence in a duodenal adenoma from an *Lrig1-CreERT2/CreERT2;Rosa26R-EYFP/EYFP* mouse that was lineage traced for 4 months from 4 weeks of age. DAPI, blue; GFP, white (to visualize EYFP). **C** and **D: Boxed regions** in **B** are magnified. Scale bars: 100 μm. Original magnification: ×5 (**C** and **D**).
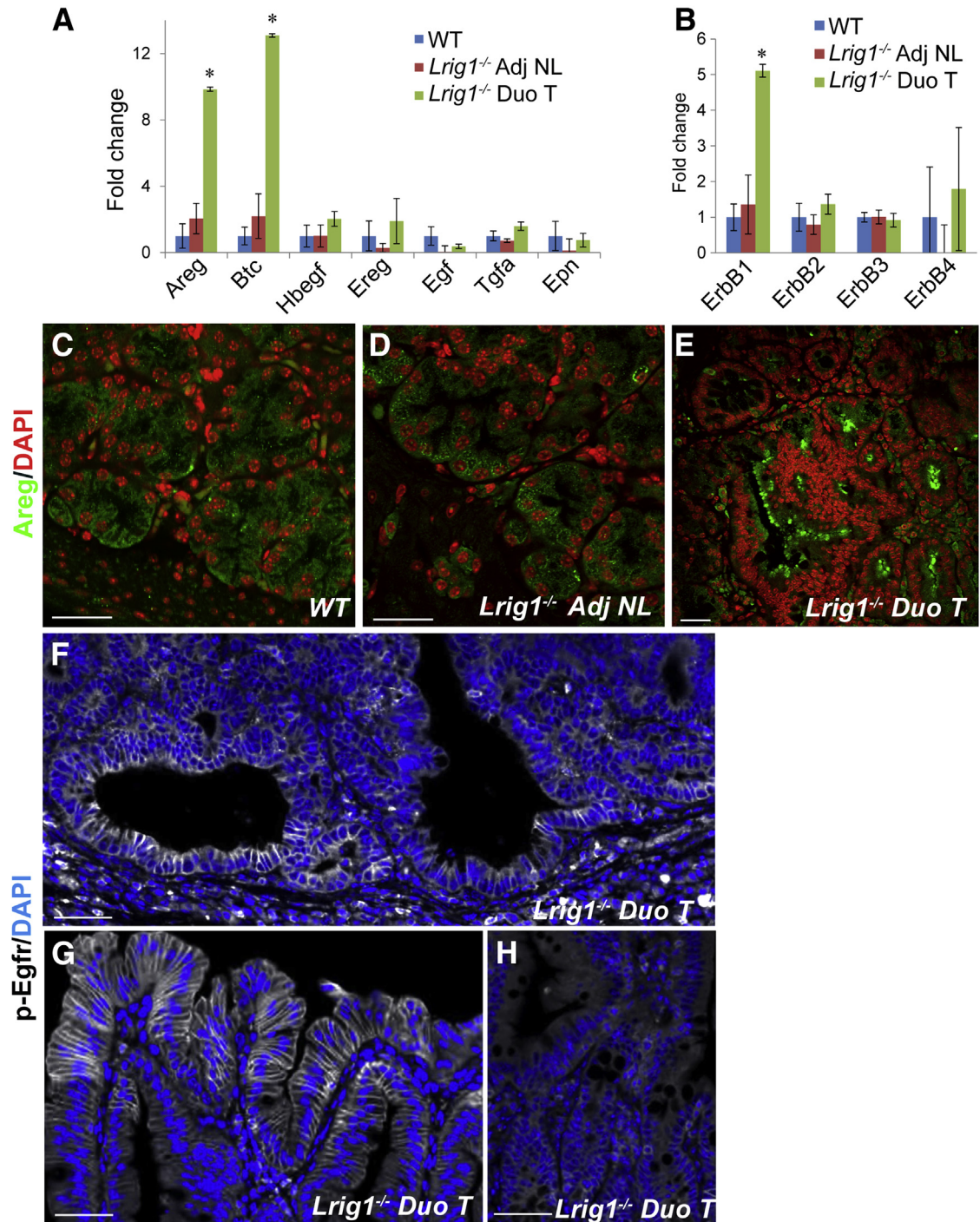
Figure 5 Duodenal adenomas (Duo Ts) in $Lrig1^{-/-}$ mice exhibit heightened epidermal growth factor receptor (Egfr) signaling. **A:** The Egfr ligands amphiregulin (Areg) and betacellulin (Btc) were up-regulated by 10- and 13-fold, respectively, in the Duo Ts by quantitative RT-PCR. **B:** Egfr is the only ErbB family member whose expression was significantly up-regulated. **C–E:** Areg immunoreactivity is similar in Brunner glands from wild-type (WT) (**C**) and $Lrig1^{-/-}$ (**D**) mice. However, Areg immunoreactivity is increased in the Duo T (**E**). **F–H:** Immunofluorescence for phosphorylated Egfr (p-Egfr) (pY1068) showed enhanced Egfr activity in an $Lrig1^{-/-}$ Duo T, both in the adenomatous region (**F**) and at the adenoma periphery (**G**); minimal signal was detected in adjacent normal (Adj NL) duodenal tissue (**H**). Confocal images were taken with the same exposure and laser voltage settings. Data are given as mean ± SEM. The unpaired Student's t-test was used on each individual transcript. *$P < 0.05$. Scale bars: 30 μm (**C–E**); 50 μm (**F–H**).

$Lrig1^{-/-}$ Duodenal Adenomas Overexpress Egfr Ligands and Have Increased Egfr Activity

Brunner glands express EGF in humans[21,22] and Egf and Tgfa in rats.[23] This prompted us to examine the expression of ErbBs and their cognate ligands in normal mouse duodenum and to compare these results with those in duodenal adenomas and adjacent normal mucosa from $Lrig1^{-/-}$ mice. We found significant up-regulation of Areg, Btc, and Egfr expression by RT-qPCR in $Lrig1^{-/-}$ duodenal adenomas
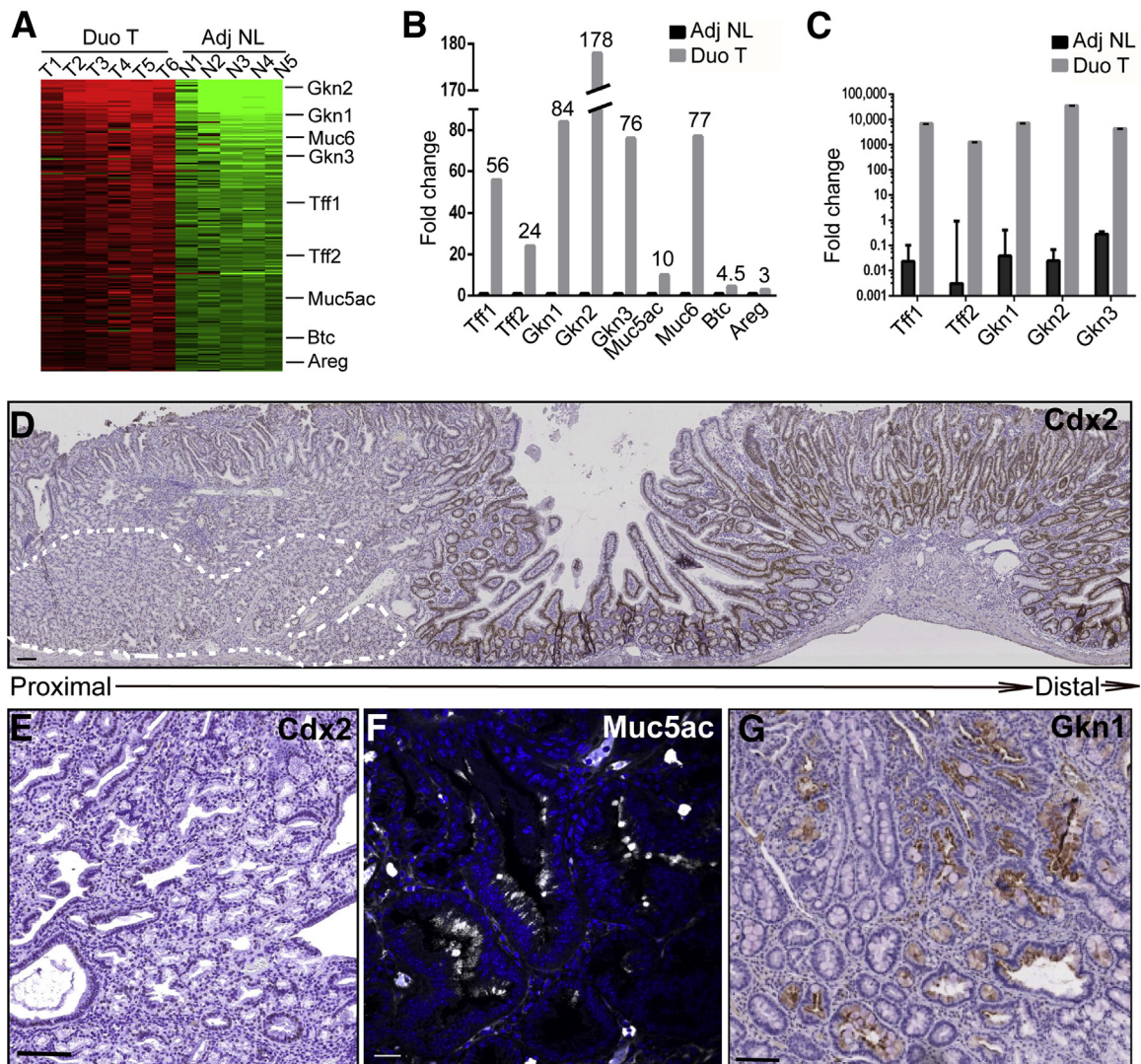
Figure 6 Duodenal adenomas (Duo Ts) in *Lrig1*^{−/−} mice express gastric-specific markers. **A:** Heat map of genes up-regulated fourfold and greater in Duo Ts compared with adjacent normal (Adj NL) tissues by gene profiling. **B:** Bar graph of the fold change in gene expression from **A**. **C:** Gastric-specific genes are significantly up-regulated by quantitative RT-PCR: *Tff1* (gastric foveolar cells), *Tff2* (antral glands and Brunner glands), *Gkn1* (gastric foveolar cells), *Gkn2* (gastric foveolar cells), and *Gkn3* (antral glands). **D:** A proximal Duo T overlying expanded Brunner glands (marked by **white dotted lines**) was largely negative for Cdx2 immunoreactivity, whereas an adjacent tubular adenoma distal to Brunner glands exhibited Cdx2 immunoreactivity. **E:** A proximal Duo T with absence of Cdx2 immunoreactivity at high power. **F** and **G:** Representative immunofluorescence for Muc5ac and immunohistochemical staining for Gkn1, indicating the presence of gastric foveolar cells in *Lrig1*^{−/−} Duo Ts. Data are given as means ± SEM. Scale bars: 100 μm (**D**, **E**, and **G**); 25 μm (**F**).

compared with grossly normal adjacent tissue and wild-type duodenum (Figure 5, A and B). Likewise, Areg immunofluorescence was more intense in *Lrig1*^{−/−} duodenal adenomas (Figure 5E and Supplemental Figure S3A) compared with wild-type duodenum (Figure 5C) and adjacent normal duodenum (Figure 5D). Areg staining intensity was similar in wild-type Brunner glands (Figure 5C) and histologically normal Brunner glands underneath *Lrig1*^{−/−} adenomas (Figure 5D). There was low, but detectable, Egf expression in the duodenum by RT-qPCR (Figure 5, A and B); however, we did not detect Egf immunoreactivity (data not shown). There was also increased p-Egfr immunoreactivity in cystically dilated glands with dysplastic cuboidal-shaped cells (Figure 5F) and at the adenoma periphery (Figure 5G)

compared with grossly normal epithelium (Figure 5H), indicating that Egfr is activated in these adenomas. Together, these data suggest that loss of *Lrig1* leads to upregulation of Egfr ligands and activation of Egfr, thus supporting a role for enhanced Egfr signaling in adenoma formation.

Lrig1^{−/−} Duodenal Adenomas Exhibit Gastric Metaplasia

To further elucidate the molecular underpinnings of *Lrig1*^{−/−} duodenal adenomas, we performed gene expression profiling of the adenomas compared with adjacent normal tissue. In addition to increased expression of Areg, Btc, and Muc6, we
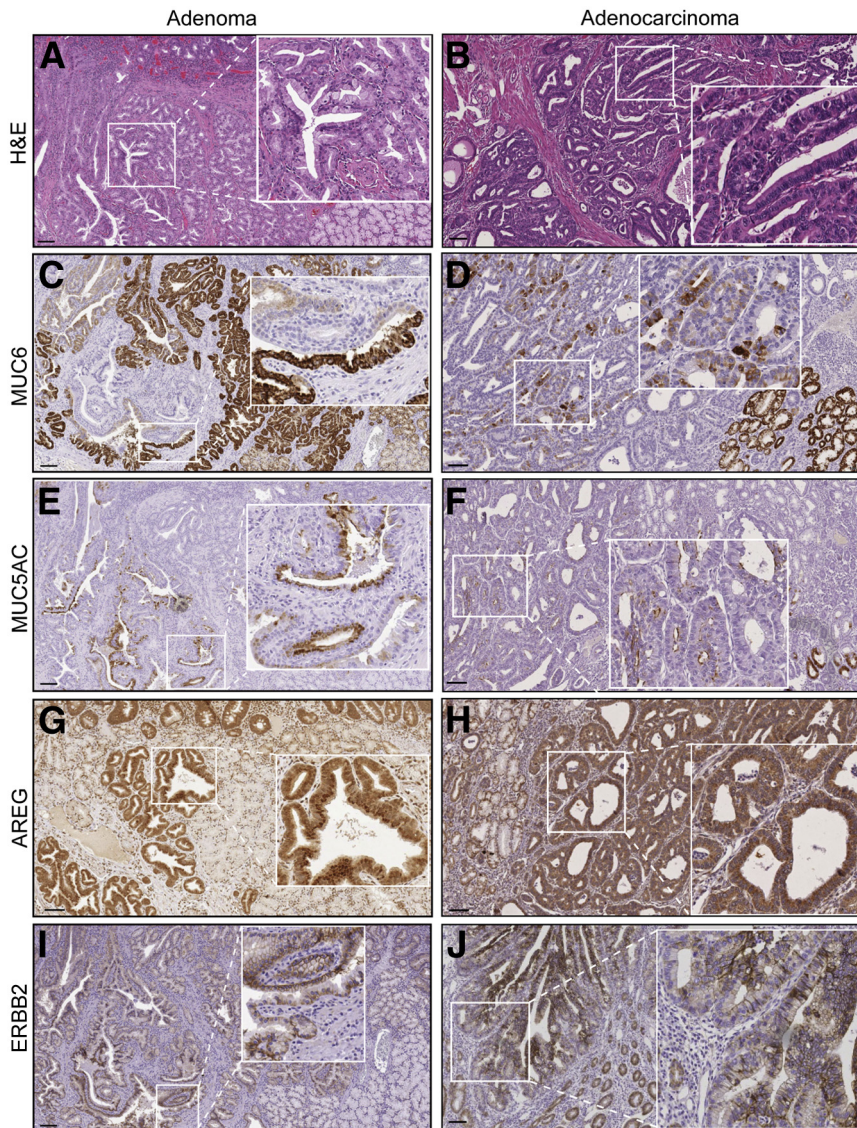
Figure 7 A subset of human duodenal tumors exhibits features of *LRIG1*$^{-/-}$ adenomas. **A** and **B:** Hematoxylin and eosin (H&E) staining of a representative human duodenal adenoma and adenocarcinoma displaying neoplastic cuboidal-shaped foveolar cells. The lesions exhibit gastric metaplasia as determined by MUC6 (**C** and **D**) and MUC5AC (**E** and **F**) staining, along with increased amphiregulin (AREG) (**G** and **H**) and ERBB2 (**I** and **J**) immunoreactivity. **Boxed regions** are magnified in **insets** (×2.5). Scale bars: 100 μm.

observed significant up-regulation of the gastric-specific markers Muc5ac, Gkn1, and trefoil factor 1 (Tff1) (Figure 6, A and B, and Supplemental Table S2). Expression of these gastric-specific genes was validated by RT-qPCR (Figure 6C). *Lrig1*$^{-/-}$ adenomas were predominantly composed of cuboidal-shaped epithelial cells resembling foveolar cells from the normal stomach that were Cdx2 negative (Figure 6, D and E) but positive for Muc5ac (Figure 6F) and Gkn1 (Figure 6G), further supporting that these adenomas exhibit gastric metaplasia. Of note, tubular adenomas distal to Brunner glands (Supplemental Figure S1, B−D) exhibited immunoreactivity for the intestinal-specific marker Cdx2 (Figure 6D and Supplemental Figure S2A).

Characterization of Gastric Metaplasia in a Subset of Human Duodenal Carcinomas

The World Health Organization has divided duodenal/ampullary carcinomas into two major groups (intestinal type and pancreatobiliary type) and five minor variants.[24] While reviewing duodenal/ampullary cancers from our institution, we identified a subset of periampullary duodenal tumors with dysplastic Brunner glands and gastric-type foveolar cells but negative CDX2 immunoreactivity (data not shown). We identified five duodenal cancers and three adenomas with these features. Similar to *LRIG1*$^{-/-}$ adenomas, we detected immunoreactivity for the gastric mucins MUC6 and MUC5AC in cuboidal neoplastic cells resembling gastric foveolar cells (Figure 7, A−F), indicating gastric metaplasia. These human tumors were also positive for AREG (Figure 7, G and H), ERBB2 (Figure 7, I and J), and p-EGFR (Figure 8, A and D), suggesting that heightened ERBB signaling may contribute to the pathogenesis of these tumors. Note that adjacent normal tissue from an adenoma and an adenocarcinoma exhibited minimal immunofluorescence (Supplemental Figure S3, B and C). Of note, LRIG1 immunoreactivity was not detected in dysplastic regions (Figure 8, B and E) but was present in adjacent normal areas

(Figure 8, C and F) and in normal human duodenum (Supplemental Figure S4). The significance of LRIG1 staining in the stroma is uncertain. The specificity of the anti-LRIG1 antibody was validated by overexpression of enhanced green fluorescent protein—tagged LRIG1 (Supplemental Figure S5). Thus, we have described a new subset of human duodenal tumors containing not only histologic features of Brunner glands and gastric metaplasia but also positive immunoreactivity for MUC6, MUC5AC, AREG, ERBB2, and p-EGFR and negative immunoreactivity for LRIG1, similar to *Lrig1*$^{-/-}$ duodenal adenomas.

Discussion

We previously reported that 14 of 16 *Lrig1*$^{-/-}$ mice (88%) developed duodenal adenomas.[18] We herein extended these studies to 54 *Lrig1*$^{-/-}$ mice and showed that duodenal adenomas occurred in 49 (91%). These findings reinforce the earlier observation that loss of *Lrig1* results in a highly penetrant adenoma phenotype and support our contention that Lrig1 acts as a tumor suppressor *in vivo*. In addition, we investigated the molecular pathogenesis of these adenomas and found that they exhibit gastric metaplasia. We propose that loss of the pan-ErbB negative regulator *Lrig1* results in increased total Egfr and p-Egfr and, in this context, predisposes to neoplasia. We identified a subset of human duodenal tumors in the periampullary region that have features of *Lrig1*$^{-/-}$ duodenal tumors, including histologically abnormal Brunner glands (hyperplastic or dysplastic), gastric metaplasia, enhanced EGFR activity, and loss of LRIG1.

Brunner glands secrete mucus to protect the duodenal mucosa from acidic and noxious contents,[20] and they produce growth factors, such as EGF[21,22] and TGFA,[23] to stimulate mucosal growth. We detected growth factors, such as Areg (Supplemental Figure S2, C and D) and p-Egfr (Supplemental Figure S2, E and F), in Brunner glands, suggesting that active Egfr signaling can support Brunner gland growth in a cell-autonomous manner. In addition, we did not observe any difference in proliferation (Supplemental Figure S2, G and H) or p-Egfr (Supplemental Figure S2, E and F) in the duodenal crypts above the Brunner glands, indicating that the overlying epithelium is less likely to contribute to increased proliferation at 4 and 5 weeks of age (Figure 2C) and increased Brunner gland size at 2 months of age (Figure 2D). Because Lrig1 is expressed in both compartments (Figure 4A), we cannot
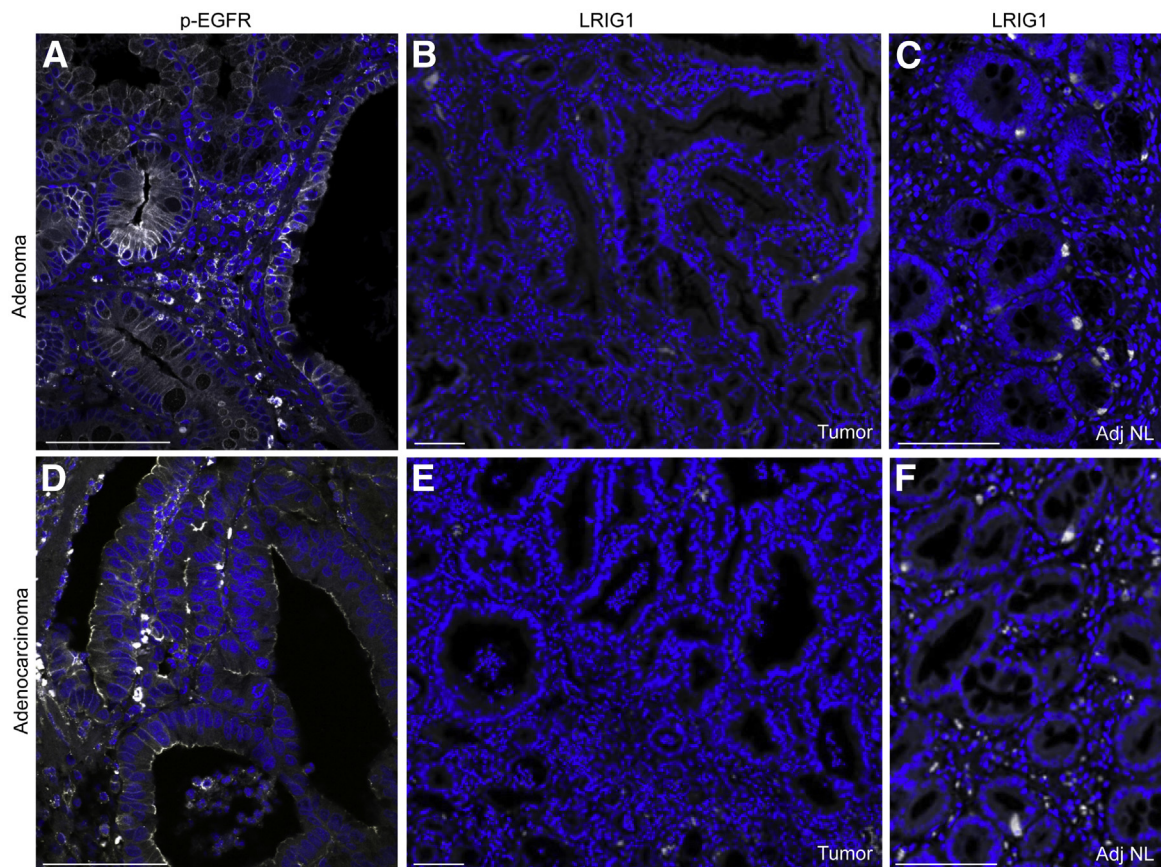
Figure 8 Human duodenal tumors exhibit enhanced epidermal growth factor receptor (EGFR) activity and loss of LRIG1. A human duodenal adenoma (**A**—**C**) and an adenocarcinoma (**D**—**F**) (histologic features are shown in Figure 7, A and B, respectively) that were positive for p-EGFR(pY1068) (**A** and **D**) but negative for LRIG1 (**B** and **E**) immunoreactivity in dysplastic regions. Adjacent normal (Adj NL) areas from an adenoma (**C**) and an adenocarcinoma (**F**) exhibited LRIG1 immunoreactivity. Scale bars: 100 μm.
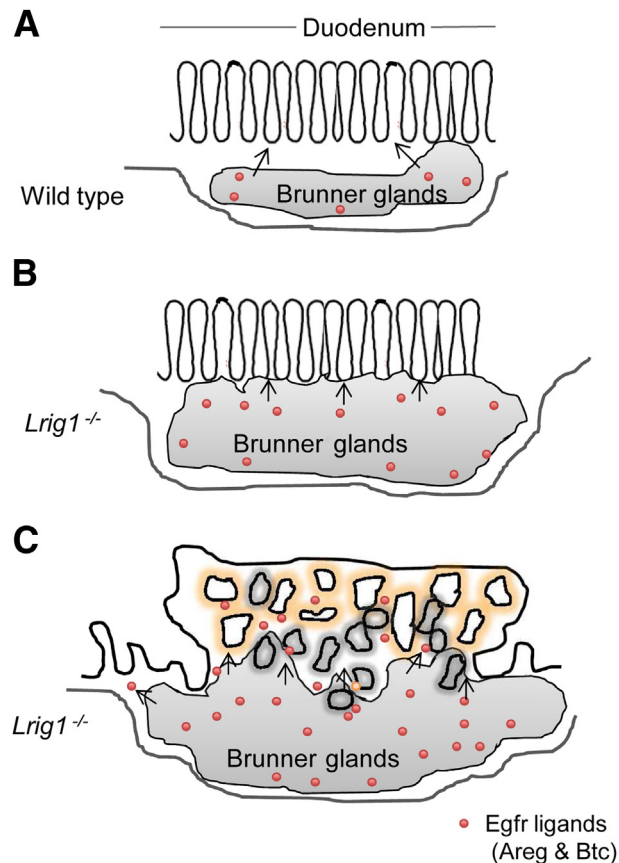
Figure 9 Schematic of a two-compartment model for duodenal adenoma formation after loss of *Lrig1*. **A:** Under normal physiologic conditions, Lrig1 maintains quiescence of progenitor cells in Brunner glands and overlying epithelium by suppressing ErbB signaling. **B:** When *Lrig1* is lost, there is increased proliferation of Brunner glands at 4 to 5 weeks of age. This enhanced proliferation results in expansion of Brunner glands by 2 months of age. The enlarged Brunner gland compartment leads to increased local production of the epidermal growth factor receptor (Egfr) ligands amphiregulin (Areg) and betacellulin (Btc). **C:** Excess Egfr ligands signal to both compartments and predispose to adenoma formation.

definitively determine the compartment from which the tumors initiate. It is also possible that loss of *Lrig1* in both compartments cooperates in adenoma formation. Further experimentation using compartment-specific driver mouse models is needed to address this issue.

During human embryonic development, MUC5AC is expressed in Brunner glands by 18 weeks of gestation, but it is lost and replaced by MUC6 by 24 weeks; this pattern of expression persists in adults.[25] Although the precise etiology is debatable,[25–27] a central element of gastric metaplasia in duodenal tissue is inflammation, often due to surface ulceration and the subsequent reparative events.[25,27–29] In response to inflammation, a reparative lineage in the mucosa differentiates into gastric foveolar-like cells.[25] This damage response recapitulates a Brunner gland developmental program, during which TFF1 and MUC5AC are expressed.[25] Whether the reparative lineage that gives rise to gastric metaplasia arises from the crypt base[25] or Brunner glands[27,30] remains to be determined.

It is thought that inflammation and ulceration can result in EGFR activation.[31,32] On genetic ablation of *Lrig1*, Egfr is activated without antecedent inflammation, and we did not observe ulceration or inflammation in *Lrig1*^{−/−} duodenal adenomas. In Lrig1 null mice, total Egfr and other ErbB receptors were increased in grossly normal intestine compared with wild-type intestine,[18] consistent with the role of Lrig1 in the down-regulation of ErbBs.[10,33–35] In addition, enhanced Egfr signaling results in transcriptional up-regulation of Egfr and its ligands (Figure 5, A and B). Thus, by *Lrig1* ablation, Egfr circumvents negative regulation; it becomes activated, thereby bypassing inflammation-associated Egfr activation. This ultimately predisposes to adenoma formation.

Based on these findings, we propose a two-compartment model in which Lrig1 acts to maintain stem cell quiescence by suppressing levels of Egfr (Figure 9). In the event of *Lrig1* loss, Egfr levels increase. Persistent proliferation due to loss of *Lrig1* leads to expansion of Brunner glands. The increase in glandular mass results in increased production of the Egfr ligands Areg and Btc. These Egfr ligands act on Egfr and other ErbBs in the overlying epithelium, predisposing to neoplasia with features of gastric metaplasia. Studies are under way to assess the requirement of Egfr in *Lrig1*^{−/−} duodenal tumorigenesis using *Egfr* conditional knockout mice (*Egfr*^{fl/fl}).

Human duodenal carcinomas are uncommon, accounting for approximately 1% of digestive cancers,[30] although most small-bowel carcinomas occur in the duodenum.[36] Most of these cases are diagnosed at an advanced stage,[37] and there is no effective treatment.[38] The two major subtypes of duodenal neoplasms are intestinal type and pancreatobiliary type. Histologically, a subset of duodenal carcinomas in the periampullary region exhibits hyperplastic or dysplastic Brunner glands and consists of atypical cuboidal-shaped columnar epithelial cells with a clear cytoplasm, resembling gastric-foveolar cells that express MUC5AC.[30] Herein, we identified a subset of human duodenal tumors with dysplastic Brunner glands, gastric metaplasia, and increased EGFR activity. In the tumors examined, LRIG1 immunoreactivity was lost in dysplastic regions (Figure 8, B and E) but retained in adjacent normal mucosa (Figure 8, C and F), as well as in normal duodenum (Supplemental Figure S4), suggesting that loss of LRIG1 may contribute to the pathogenesis of this tumor type. However, note that there are many ways to increase ERBB activity, including mutation or amplification of receptors, increased EGFR ligands, and loss of negative regulators. Thus, multiple pathogenic mechanisms other than loss of LRIG1 could result in enhanced EGFR activity, ultimately leading to cancer.

Acknowledgments

providing Tff2 RT-qPCR primers, Joseph Roland and the Vanderbilt Digital Histology Shared Resource for automated imaging, and Frank Revetta for immunohistochemical support.

Supplemental Data

Supplemental material for this article can be found at *http://dx.doi.org/10.1016/j.ajpath.2014.12.014*.

References

1. Lemmon MA, Schlessinger J: Cell signaling by receptor tyrosine kinases. Cell 2010, 141:1117−1134
2. Hynes NE, MacDonald G: ErbB receptors and signaling pathways in cancer. Curr Opin Cell Biol 2009, 21:177−184
3. Fiske WH, Threadgill D, Coffey RJ: ERBBs in the gastrointestinal tract: recent progress and new perspectives. Exp Cell Res 2009, 315:583−601
4. Singh B, Bogatcheva G, Washington MK, Coffey RJ: Transformation of polarized epithelial cells by apical mistrafficking of epiregulin. Proc Natl Acad Sci U S A 2013, 110:8960−8965
5. Barnard JA, Graves-Deal R, Pittelkow MR, DuBois R, Cook P, Ramsey GW, Bishop PR, Damstrup L, Coffey RJ: Auto- and cross-induction within the mammalian epidermal growth factor-related peptide family. J Biol Chem 1994, 269:22817−22822
6. Coffey RJ Jr, Derynck R, Wilcox JN, Bringman TS, Goustin AS, Moses HL, Pittelkow MR: Production and auto-induction of transforming growth factor-alpha in human keratinocytes. Nature 1987, 328:817−820
7. Hanahan D, Weinberg RA: Hallmarks of cancer: the next generation. Cell 2011, 144:646−674
8. Gotoh N: Feedback inhibitors of the epidermal growth factor receptor signaling pathways. Int J Biochem Cell Biol 2009, 41:511−515
9. Wang Y, Poulin EJ, Coffey RJ: LRIG1 is a triple threat: ERBB negative regulator, intestinal stem cell marker and tumour suppressor. Br J Cancer 2013, 108:1765−1770
10. Gur G, Rubin C, Katz M, Amit I, Citri A, Nilsson J, Amariglio N, Henriksson R, Rechavi G, Hedman H, Wides R, Yarden Y: LRIG1 restricts growth factor signaling by enhancing receptor ubiquitylation and degradation. EMBO J 2004, 23:3270−3281
11. Thompson PA, Ljuslinder I, Tsavachidis S, Brewster A, Sahin A, Hedman H, Henriksson R, Bondy ML, Melin BS: Loss of LRIG1 locus increases risk of early and late relapse of stage I/II breast cancer. Cancer Res 2014, 74:2928−2935
12. Miller JK, Shattuck DL, Ingalla EQ, Yen L, Borowsky AD, Young LJ, Cardiff RD, Carraway KL 3rd, Sweeney C: Suppression of the negative regulator LRIG1 contributes to ErbB2 overexpression in breast cancer. Cancer Res 2008, 68:8286−8294
13. Lindstrom AK, Ekman K, Stendahl U, Tot T, Henriksson R, Hedman H, Hellberg D: LRIG1 and squamous epithelial uterine cervical cancer: correlation to prognosis, other tumor markers, sex steroid hormones, and smoking. Int J Gynecol Cancer 2008, 18:312−317
14. Tanemura A, Nagasawa T, Inui S, Itami S: LRIG-1 provides a novel prognostic predictor in squamous cell carcinoma of the skin: immunohistochemical analysis for 38 cases. Dermatol Surg 2005, 31:423−430
15. Lindquist D, Kvarnbrink S, Henriksson R, Hedman H: LRIG and cancer prognosis. Acta Oncol 2014, 53:1135−1142
16. Johansson M, Oudin A, Tiemann K, Bernard A, Golebiewska A, Keunen O, Fack F, Stieber D, Wang B, Hedman H, Niclou SP: The soluble form of the tumor suppressor Lrig1 potently inhibits in vivo glioma growth irrespective of EGF receptor status. Neuro Oncol 2013, 15:1200−1211
17. Qi XC, Xie DJ, Yan QF, Wang YR, Zhu YX, Qian C, Yang SX: LRIG1 dictates the chemo-sensitivity of temozolomide (TMZ) in U251 glioblastoma cells via down-regulation of EGFR/topoisomerase-2/Bcl-2. Biochem Biophys Res Commun 2013, 437:565−572
18. Powell AE, Wang Y, Li Y, Poulin EJ, Means AL, Washington MK, Higginbotham JN, Juchheim A, Prasad N, Levy SE, Guo Y, Shyr Y, Aronow BJ, Haigis KM, Franklin JL, Coffey RJ: The pan-ErbB negative regulator Lrig1 is an intestinal stem cell marker that functions as a tumor suppressor. Cell 2012, 149:146−158
19. Edgar R, Domrachev M, Lash AE: Gene Expression Omnibus: NCBI gene expression and hybridization array data repository. Nucleic Acids Res 2002, 30:207−210
20. Krause WJ: Brunner's glands: a structural, histochemical and pathological profile. Prog Histochem Cytochem 2000, 35:259−367
21. Poulsen SS, Nexo E, Olsen PS, Hess J, Kirkegaard P: Immunohistochemical localization of epidermal growth factor in rat and man. Histochemistry 1986, 85:389−394
22. Kirkegaard P, Olsen PS, Poulsen SS, Nexo E: Exocrine secretion of epidermal growth factor from Brunner's glands. stimulation by VIP and acetylcholine. Regul Pept 1983, 7:367−372
23. Hormi K, Onolfo JP, Gres L, Lebraud V, Lehy T: Developmental expression of transforming growth factor-alpha in the upper digestive tract and pancreas of the rat. Regul Pept 1995, 55:67−77
24. Shepherd N, Carr N, Howe J, Noffsinger A, Warren B: Tumors of the small intestine. Edited by Bosman FT, Carneiro F, Hruban RH, Theise ND. WHO Classification of Tumours of the Digestive System, ed 4. Lyon, International Agency for Research on Cancer, 2010, pp 98−101
25. Ahnen DJ, Poulsom R, Stamp GW, Elia G, Pike C, Jeffery R, Longcroft J, Rio MC, Chambon P, Wright NA: The ulceration-associated cell lineage (UACL) reiterates the Brunner's gland differentiation programme but acquires the proliferative organization of the gastric gland. J Pathol 1994, 173:317−326
26. Shaoul R, Marcon P, Okada Y, Cutz E, Forstner G: The pathogenesis of duodenal gastric metaplasia: the role of local goblet cell transformation. Gut 2000, 46:632−638
27. Kushima R, Manabe R, Hattori T, Borchard F: Histogenesis of gastric foveolar metaplasia following duodenal ulcer: a definite reparative lineage of Brunner's gland. Histopathology 1999, 35:38−43
28. Gormally SM, Kierce BM, Daly LE, Bourke B, Carroll R, Durnin MT, Drumm B: Gastric metaplasia and duodenal ulcer disease in children infected by Helicobacter pylori. Gut 1996, 38:513−517
29. Shousha S, Parkins RA, Bull TB: Chronic duodenitis with gastric metaplasia: electron microscopic study including comparison with normal. Histopathology 1983, 7:873−885
30. Kushima R, Stolte M, Dirks K, Vieth M, Okabe H, Borchard F, Hattori T: Gastric-type adenocarcinoma of the duodenal second portion histogenetically associated with hyperplasia and gastric-foveolar metaplasia of Brunner's glands. Virchows Arch 2002, 440:655−659
31. Tarnawski AS, Ahluwalia A: Molecular mechanisms of epithelial regeneration and neovascularization during healing of gastric and esophageal ulcers. Curr Med Chem 2012, 19:16−27
32. Sinha A, Nightingale J, West KP, Berlanga-Acosta J, Playford RJ: Epidermal growth factor enemas with oral mesalamine for mild-to-moderate left-sided ulcerative colitis or proctitis. N Engl J Med 2003, 349:350−357
33. Ledda F, Bieraugel O, Fard SS, Vilar M, Paratcha G: Lrig1 is an endogenous inhibitor of Ret receptor tyrosine kinase activation, downstream signaling, and biological responses to GDNF. J Neurosci 2008, 28:39−49
34. Shattuck DL, Miller JK, Laederich M, Funes M, Petersen H, Carraway KL III, Sweeney C: LRIG1 is a novel negative regulator of the Met receptor and opposes Met and Her2 synergy. Mol Cell Biol 2007, 27:1934−1946

35. Laederich MB, Funes-Duran M, Yen L, Ingalla E, Wu X, Carraway KL 3rd, Sweeney C: The leucine-rich repeat protein LRIG1 is a negative regulator of ErbB family receptor tyrosine kinases. J Biol Chem 2004, 279:47050−47056

36. Ohta Y, Saitoh K, Akai T, Uesato M, Ochiai T, Matsubara H: Early primary duodenal carcinoma arising from Brunner's glands synchronously occurring with sigmoid colon carcinoma: report of a case. Surg Today 2008, 38:756−760

37. Kawamoto K, Motooka M, Hirata N, Masuda K, Ueyama T, Yasukouchi A, Iwashita A, Matsuzawa K, Katsuyama T: Early primary carcinoma of the duodenal bulb arising from Brunner's glands. Gastrointest Endosc 1994, 40: 233−236

38. Kitagori K, Miyamoto S, Sakurai T: Image of the month. adenocarcinoma derived from Brunner's gland. Clin Gastroenterol Hepatol 2010, 8:A26